Asian Journal of Chemistry; Vol. 31, No. 3 (2019), 566-568

ASIAN JOURNAL OF CHEMISTRY

https://doi.org/10.14233/ajchem.2019.21685

Synthesis and Characterization of Cobalt(II) Complexes with Hemilabile P^N Donor Ligands

RAJJYOTI GOGOI*, CHANDAN PATHAK and GEETIKA BORAH

Department of Chemistry, Dibrugarh University, Dibrugarh-786004, India

*Corresponding author: E-mail: rajjyotigogoi99@gmail.com

Received: 30 August 2018; *Accepted*: 24 October 2018; *Published online*: 31 January 2019; AJC-19246

Two cobalt(II) complexes *viz.* $CoCl_2\{PPh_2(p\text{-}C_6H_4NMe_2)\}_2$ (**C**$_1$) and $CoCl_2(PPh_2Py)_2$ (**C**$_2$) were synthesized by reacting $CoCl_2{\cdot}6H_2O$ and 4-(dimethylamino)phenyldiphenylphosphine and diphenyl-2-pyridylphosphine ligands, respectively. The complexes were characterized by elemental analysis, FT-IR, UV-visible and electronic spin resonance (ESR) spectroscopic technique. Both the complexes were found stable at room temperature. EPR measurements and UV-visible spectra analysis of **C**$_1$ and **C**$_2$ are consistent with a tetrahedral Co(II) and tetragonally distorted octahedral Co(II) ions, respectively.

Keywords: Cobalt, Ligand, 4-(Dimethylamino)phenyldiphenylphosphine, Diphenyl-2-pyridylphosphine, Tetragonal.

INTRODUCTION

Transition metal complexes containing hemilabile ligand have received considerable attention because of their unusual structural features, versatile binding modes and biological implications [1-7]. Different types of hemilabile ligands such as P-O, P-S, P-N *etc*. and their transition metal complexes have been reported. Hemilabile ligands have several distinct advantages over the homo functional ligands [8,9]. Aminophosphines can make the metal centre more electron rich by direct M-P or M-N interaction. Due to this reason they have greater ability to undergo oxidative addition and reductive elimination reactions and found tremendous catalytic applications in homo and heterogeneous systems for different reactions such as hydrogenation, hydroformylation, carbonylation, transfer hydrogenation, cross-coupling reaction *etc*. [10-17]. It can bind to the metal atom in a number of fashions depending upon the structure of the ligand and the oxidation state of the metal. The P-donor can stabilize the metal in their low oxidation state, while N-donor can create a vacant coordination site for substrate binding. These ligands have important applications in supramolecular chemistry also.

Aydemir and co-workers [1] have reported Rh(I), Ru(II), Ir(III) complexes of aminophosphines and found promising catalytic activity in transfer hydrogenation reaction. The phosphinoamine chemistry of 4*d*- and 5*d*-transition metals are more developed than the 3*d*-transition metal ions, probably because of the large size of these atoms. Few monodentate and bidentate cobalt complexes of P^N ligands have been reported which exhibited diverse steric and electronic properties [18,19]. Some of them have rigid back bond and some other have flexible alkyl chain that join the two/three donor atoms. Moreover, few complexes of Fe, Au, Ag and W with diphenyl-2-pyridylphosphine and 4-(dimethylamino)phenyldiphenylphosphine ligands have also been reported [20-23]. Our interest in the present work is to extend the boundary-line of the phosphinoamine chemistry towards 1st row transition metals and herein we report the synthesis of Co(II) complexes with 4-(dimethylamino)phenyldiphenylphosphine and diphenyl-2-pyridylphosphine ligands and characterization of these complexes.

EXPERIMENTAL

All the reagents used in the synthesis of the complexes were of AR grade. The metal precursor ($CoCl_2{\cdot}6H_2O$) was used without further purification. All organic solvents such as ethanol, DCM, DMSO *etc.* used in the present work were purchased from Merck and were distilled according to standard procedure. The ligands, diphenyl-2-pyridylphosphine and 4-(dimethylamino)-phenyldiphenylphosphine were purchased from Sigma Aldrich and used as received.

FT-IR spectra were recorded in KBr pellets on Shimadzu IR prestige-21 FT-IR spectrophotometer (4000-200 cm^{-1}). The

This is an open access journal, and articles are distributed under the terms of the Creative Commons Attribution-NonCommercial-ShareAlike 4.0 (CC BY-NC-SA 4.0) International License which allows readers to freely read, download, copy, distribute, print, search, or link to the full texts of its articles and to use them for any other lawful non-commercial purpose as long as the original source is duly acknowledged.

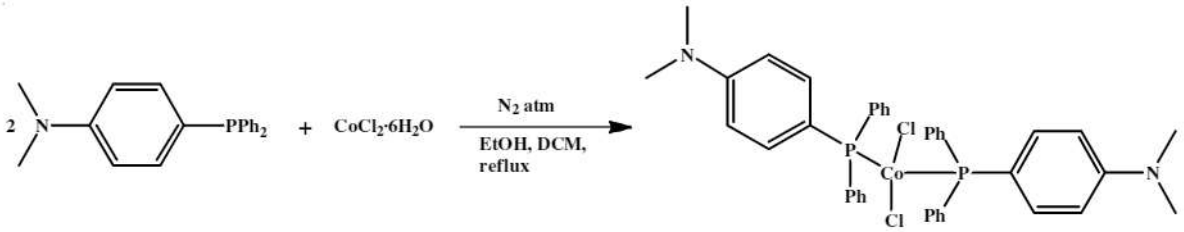

Scheme-I: Synthesis of the complex $[CoCl_2\{PPh_2(p\text{-}C_6H_4NMe_2)\}_2]$ ($\mathbf{C_1}$)

ESR spectra of the complexes were recorded at liquid nitrogen temperature in X-band region at IIT, Madras, India. The electronic spectra of the complexes were recorded in DCM solution in the range 200-800 nm with a Graphicord UV-240 (Shimadzu), UV-1700 spectrophotometer. ^1H and ^{31}P NMR were recorded in DMSO-d_6 using TMS as an internal standard on a Brucker Avance 400 MHz spectrometer. The C, H and N analysis were done with a Perkin-Elmer 2400 Series II C,H,N analyzer. Melting point of the complexes were recorded with a Buchi B 450 melting point apparatus.

Synthesis of $[CoCl_2\{PPh_2(p\text{-}C_6H_4NMe_2)\}_2]$ ($\mathbf{C_1}$): 1 mmol (0.51 g) $CoCl_2{\cdot}6H_2O$ dissolved in 10 mL ethanol was added to a solution of 4-(dimethylamino)phenyldiphenylphosphine prepared by dissolving 2 mmol (0.84 g) of the ligand in 10 mL DCM. The reaction mixture was then refluxed under N_2 atm for 3 h with constant stirring. The resulting mixture was evaporated under reduced pressure whereupon a solid mass was obtained (**Scheme-I**). It was washed with ether and dried. Finally a dark green solid was obtained. Found (calcd.): C, 66.52 (67.17); H, 5.40 (5.74); N, 4.07 (3.71) for $CoCl_2\{PPh_2(p\text{-}C_6H_4NMe_2)\}_2$. m.p. 161 °C. IR (KBr, ν_{max}, cm^{-1}): 1436 (C-N), 432 (Co-P), 343 (Co-Cl).

Synthesis of $[CoCl_2(PPh_2Py)_2]$ ($\mathbf{C_2}$): 2 mmol (0.53 g) Diphenyl-2-pyridylphosphine and 1 mmol (0.51 g) $CoCl_2{\cdot}6H_2O$ was dissolved separately in 10 mL DCM and 10 mL ethanol, respectively and was mixed slowly with stirring. The reaction mixture was refluxed for 3 h with constant stirring under N_2 atmosphere. The solvent was then evaporated under vacuum and the resulting solid mass was washed with ether and dried in vacuum (**Scheme-II**). Finally a dark green solid was obtained. Found (calcd.) C, 63.05 (62.99); H, 4.1 (4.99); N, 3.91 (4.08) for $CoCl_2(PPh_2Py)_2$. m.p. 154 °C. IR (KBr, ν_{max}, cm^{-1}): 1431 (py(C=N)), 520 (Co-N), 440 (Co-P), 332 (Co-Cl).

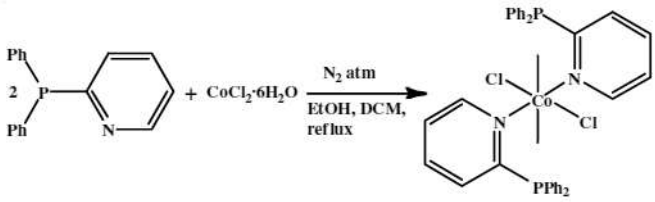

Scheme-II: Synthesis of the complex $[CoCl_2(PPh_2Py)_2]$ ($\mathbf{C_2}$)

RESULTS AND DISCUSSION

The melting point of the complexes $\mathbf{C_1}$ and $\mathbf{C_2}$ are found to be 161 °C and 154 °C, respectively, which are different from the melting point of the starting materials $CoCl_2{\cdot}6H_2O$ (m.p.: 110 °C) and the respective ligands $PPh_2(p\text{-}C_6H_4NMe_2)$ (d.p. 151-154 °C) and PPh_2Py (m.p.: 85 °C), indicating the formation of the new complexes $\mathbf{C_1}$ and $\mathbf{C_2}$. The complexes are dark green in colour and soluble in common organic solvents *viz.* dichloromethane, tetrahydrofuran, DMSO *etc*. and were found stable under ambient conditions.

FT-IR study: The ν(C-N) stretching frequency for the complex, $\mathbf{C_1}$ was observed at 1436 cm^{-1} which was almost equal to the ν(C-N) stretching frequency value of the free ligand, indicating that the $-NMe_2$ did not take part in the complexation. A weak band at 432 cm^{-1} and a moderate intensity band at 343 cm^{-1} could be assigned to Co-P and Co-Cl stretching vibrations, respectively [5]. In the IR spectrum of $\mathbf{C_2}$ a sharp band at 1431 cm^{-1} was attributed to the ν_{py}(C=N) vibration. This band showed a significant downfield shift compared to the free ligand PPh_2Py, indicated coordination through N-atom. The complex $\mathbf{C_2}$ exhibited moderate intensity peaks at 520, 440 and 332 cm^{-1} attributable to Co-N, Co-P and Co-Cl vibrations, respectively [3,4].

UV-visible spectral analysis: In the UV-visible spectrum of complex $\mathbf{C_1}$ (Fig. 1a) an absorption at 405 nm could be assigned to intra ligand $n\rightarrow\pi^*$ transition. The bands at 720 and 632 nm could be tentatively attributed to $^4A_2(F) \rightarrow {}^4T_1(F)$ and $^4A_2(F) \rightarrow {}^4T_1(P)$ transitions, respectively. The splitting of peak at 632 nm may be due to distortion from regular symmetry. The complex $\mathbf{C_2}$ demonstrated two peaks at 650 and 587 nm assignable to the transitions $^4T_{1g}(F) \rightarrow {}^4A_{2g}(F)$ and $^4T_{1g}(F) \rightarrow {}^4T_{1g}(P)$, respectively (Fig. 1b). Appearance of a hump peak at 700 nm clearly indicates Jahn-Teller distortion in the complex [24]. UV-visible spectral analysis indicates distorted tetrahedral geometry and octahedral geometry (Jahn-Teller distortion) for the complexes $\mathbf{C_1}$ and $\mathbf{C_2}$, respectively.

ESR analysis: The ESR spectra of both complexes $\mathbf{C_1}$ and $\mathbf{C_2}$ were recorded at liquid N_2 temperature in magnetically dilute form. The complex $\mathbf{C_1}$ exhibited three g values at 4.91, 3.62 and 2.45, which is attributed to tetrahedral symmetry around the metal ion. A tetrahedral Co(II) would result in a ground S = 3/2 state, so is a Kramers ion and due to zero field splitting should show three EPR signals (Fine splitting) [25]. On the other hand, two g values at 2.77 ($g_{\parallel}$) and 1.83 ($g_{\perp r}$) for the complex $\mathbf{C_2}$ is indicative of tetragonally distorted octahedral environment around the cobalt ion [26].

(^{1}H and ^{31}P) NMR analysis: Since the complexes are paramagnetic, so their NMR spectra could not be resolved.

Conclusion

We have successfully synthesized monometallic two Co(II) complexes of the rigid backbone 4-(dimethylamino)-phenyldiphenylphosphine and flexible diphenyl-2-pyridylphosphine ligands. The complexes $\mathbf{C_1}$ and $\mathbf{C_2}$ were tentatively assigned a tetrahedral and tetragonally distorted octahedral geometry, respectively.

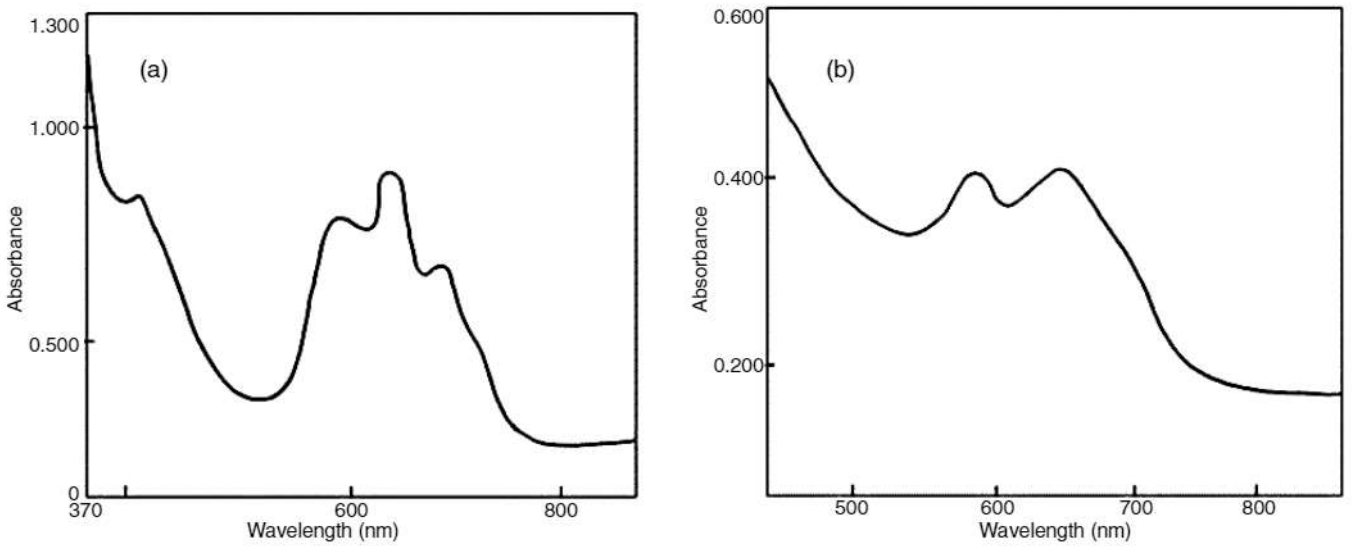

Fig. 1. Electronic absorption spectrum of (a) $CoCl_2\{PPh_2(p\text{-}C_6H_4NMe_2)\}_2$ (**C₁**) and (b) $CoCl_2(PPh_2Py)_2$ (**C₂**) complexes

ACKNOWLEDGEMENTS

The authors gratefully acknowledge the services of IIT, Madras for EPR spectra and SAIF, NEHU, Shillong for NMR facilities. The authors are thankful to UGC, New Delhi, India for financial support under the SAD-DRS-I program (2016-2021).

CONFLICT OF INTEREST

The authors declare that there is no conflict of interests regarding the publication of this article.

REFERENCES

1. M. Aydemir, A. Baysal and Y. Turgut, *Appl. Organomet. Chem.*, **25**, 270 (2011); https://doi.org/10.1002/aoc.1753.
2. P. Das, P.P. Sarmah, M. Borah and A.K. Phukan, *Inorg. Chim. Acta*, **362**, 5001 (2009); https://doi.org/10.1016/j.ica.2009.08.006.
3. G. Borah and D. Boruah, *Indian J. Chem.*, **51A**, 444 (2012).
4. G. Borah and D. Boruah, *Indian J. Chem.*, **52A**, 334 (2013).
5. G. Borah, D. Boruah, G. Sarmah, S.K. Bharadwaj and U. Bora, *Appl. Organometal. Chem.*, **27**, 688 (2013); https://doi.org/10.1002/aoc.3029.
6. G. Borah, P.P. Sarmah and D. Boruah, *Bull. Korean Chem. Soc.*, **36**, 1226 (2015); https://doi.org/10.1002/bkcs.10237.
7. D. Sahu, B. Banik, M. Borah and P. Das, *Lett. Org. Chem.*, **11**, 671 (2014); https://doi.org/10.2174/15701786116661406172136 20.
8. J.J. Fernández, A. Fernández, D. Vázquez-Garcia, M. López-Torres, A. Suárez and J.M. Vila, *Polyhedron*, **26**, 4567 (2007); https://doi.org/10.1016/j.poly.2007.06.012.
9. P. Braunstein and F. Naud, *Angew. Chem. Int. Ed.*, **40**, 680 (2001); https://doi.org/10.1002/1521-3773(20010216)40:4<680::AID-ANIE6800>3.0.CO;2-0.
10. J. Zhang, G. Leitus, Y. Ben-David and D. Milstein, *Angew. Chem.*, **118**, 1131 (2006); https://doi.org/10.1002/ange.200503771.
11. F.E. Hahn, M.C. Jahnke and T. Pape, *Organometallics*, **25**, 5927 (2006); https://doi.org/10.1021/om060741u.
12. R. Sharma, M. Chouhan, D. Sood and V.A. Nair, *Appl. Organomet. Chem.*, **25**, 305 (2011); https://doi.org/10.1002/aoc.1759.
13. P. Braunstein, *J. Org. Chem.*, **689**, 3953 (2004); https://doi.org/10.1016/j.jorganchem.2004.06.024.
14. C. Gunanathan, B. Gnanaprakasam, M.A. Iron, L.J.W. Shimon and D. Milstein, *J. Am. Chem. Soc.*, **132**, 14763 (2010); https://doi.org/10.1021/ja107770y.
15. V. Leigh, W. Ghattas, H. Mueller-Bunz and M. Albrecht, *J. Org. Chem.*, **771**, 33 (2014); https://doi.org/10.1016/j.jorganchem.2014.05.022.
16. J.P. Tassone and G.J. Spivak, *J. Organomet. Chem.*, **841**, 57 (2017); https://doi.org/10.1016/j.jorganchem.2017.04.012.
17. T. Nakajima, S. Kurai, S. Noda, M. Zouda, B. Kure and T. Tanase, *Organometallics*, **31**, 4283 (2012); https://doi.org/10.1021/om300278k.
18. M. Muranaka, I. Hyodo, W. Okumura and T. Oshiki, *Catal. Today*, **164**, 552 (2011); https://doi.org/10.1016/j.cattod.2010.11.050.
19. S.L. Queiroz, A.A. Batista, M.P. de Araujo, R.C. Bianchini, G. Oliva, J. Ellena and B.R. James, *Can. J. Chem.*, **81**, 1263 (2003); https://doi.org/10.1139/v03-109.
20. A. Dervisi, P.G. Edwards, P.D. Newman and R.P. Tooze, *J. Chem. Soc., Dalton Trans.*, 523 (2000); https://doi.org/10.1039/a908050c.
21. S.J. Coles, S.E. Durran, M.B. Hursthouse, A.M.Z. Slawin and M.B. Smith, *New J. Chem.*, **25**, 416 (2001); https://doi.org/10.1039/b008502m.
22. C. Tejel, M.A. Ciriano, R. Bravi, L.A. Oro, C. Graiff, R. Galassi and A. Burini, *Inorg. Chim. Acta*, **347**, 129 (2003); https://doi.org/10.1016/S0020-1693(02)01447-0.
23. O.N. Temkin and L.G. Bruk, *Kinet. Katal.*, **44**, 661 (2003) (in Russian).
24. D. Sutton, Electronic Spectra of Transition Metal Complexes, McGraw-Hill: London (1968).
25. A. Romerosa, C. Saraiba-Bello, M. Serrano-Ruiz, A. Caneschi, V. McKee, M. Peruzzini, L. Sorace and F. Zanobini, *Dalton Trans.*, 3233 (2003); https://doi.org/10.1039/b305443h.
26. R.L. Dutta and S. Syamal, Elements of Magnetochemistry, Affiliated East-West Press: New Delhi, edn 2 (1993).

Journal of Organometallic Chemistry 897 (2019) 80–88

Contents lists available at ScienceDirect

Journal of Organometallic Chemistry

journal homepage: www.elsevier.com/locate/jorganchem

Agro waste derived nanosilica supported Pd(ll) complex: A protocol for copper free Sonogashira reaction in water

Rajjyoti Gogoi, Rituraj Saikia, Geetika Borah*

Department of Chemistry, Dibrugarh University, Dibrugarh, Assam, India

ARTICLE INFO

Article history:
Received 7 December 2018
Received in revised form
11 June 2019
Accepted 14 June 2019
Available online 24 June 2019

Keywords:
Aliphatic alkyne
Aryl halide
Diaryl alkyne
Sonogashira cross-coupling
Terminal alkyne
Thermogravimetric

ABSTRACT

A palladium (II) complex immobilized onto nanosilica(Pd-imine@nanoSiO$_2$) has been developed and evaluated as a highly efficient, retrievable catalyst for carbon-carbon triple bond activation reactions between aryl halides and terminal alkynes. Nanosilica has been derived from rice husk by simple and eco-compatible methodology. The catalyst has been extensively characterized by techniques such as FT-IR, UV—vis, powder XRD, XPS, SEM-EDX, thermogravimetric analysis, BET surface area measurement. The catalyst can be reused for five consecutive runs without compromising much with the activity. Easy preparation, its long shelf life, air-stability, wide substrate scope, 'in water' reactions, easy separability and good recyclability make it an ideal system for Sonogashira cross-coupling reaction. Moreover, various alkyne substrates were efficiently cross-coupled with a broad range of aryl iodides and aryl bromides to afford diaryl alkynes, providing improved yields with low catalyst loading in water. This protocol is also suitable for aliphatic alkynes.

© 2019 Elsevier B.V. All rights reserved.

1. Introduction

Sonogashira reaction belongs to the most powerful tool for the construction of C(sp)-C(sp^2) bond allowing the synthesis of different acetylene derivatives such as, pharmaceuticals, polymers, dyes, sensors, etc. [1—4]. The acetylene derivatives find tremendous applications in material chemistry due to their unique electrical and optical properties. Therefore, remarkable efforts have been devoted to improve the synthetic methodologies of the reaction and also to increase its efficiency. Traditionally, this reaction was catalyzed by palladium salt in the presence of different ligands *viz.* phosphine based, N-based, Schiff-base, etc. along with a copper co-catalyst in an amine as a solvent. In the recent decades, however, several copper-free Sonogashira reaction methodologies have been proposed, since from environmental perspectives copper-mediated protocol is no longer viable as it produces a significant amount of unwanted homo coupling product of the terminal alkynes along with the desired product and needs an extra non environment friendly chemical CuX [5—10]. As a result several alternative methodologies were proposed time to time including designing of different ligand systems, use of additives, *viz.* tetra-n-butylammonium salt, sodium sulphide, Ag, Zn etc. However, most of these protocols were homogeneous in nature with advantages of higher yields but with distinct drawbacks like non-reusability, contamination of the products, catalyst loss and tedious workup procedures. These prompted researchers to develop ecofriendly, cheap and reusable heterogeneous systems [11].Till now various heterogeneous catalysts such as silica, clay, zeolites and SBA-15 immobilized Pd complex/Pd(0)nanoparticles; bimetallic Pd-nanoparticles; polymer-supported N-heterocyclic carbene—palladium catalyst; poly(vinyl chloride)-supported Pd(II) complex; Pd(II) Schiff-base complex supported on multiwalled carbon nanotubes; Pd(II) supported on MCM-41 were reported for Sonogashira reactions [12—16].Although significant advancements have been made, as per our literature review bio-derived silica supported Pd(II) complex has not been reported as catalyst for Sonogashira reaction till date. However, because of some specific characteristics like low cost, wide availability, high thermal stability and surface reactivity, high surface area, silica is one of the best candidates as solid support material [17—22]. Silica is found in various natural sources with different proportions. Agro waste such as rice husk ash is one of the cheapest and most eco-friendly sources of silica with 90—97% silica content [23].So extraction of silica particle from rice husk ash benefits not only of producing valuable silica powder but also of reducing disposal and pollution problems.

* Corresponding author.
E-mail address: geetikachem@yahoo.co.in (G. Borah).

https://doi.org/10.1016/j.jorganchem.2019.06.015
0022-328X/© 2019 Elsevier B.V. All rights reserved.

Recently we have reported the efficiency of rice husk derived nanosilica supported Pd(II) and Ru(III) complexes and montmorillonite K-10 supported Pd(0) nanoparticles in Suzuki–Miyaura, hydration of nitriles and selective oxidation of benzyl alcohols reactions, respectively [23,24]. So in order to extend the scope of bio-derived nanosilica anchored Pd(II) complex, here we have reported a simple and efficient protocol for the Sonogashira reaction of aryl iodides in water under mild conditions.

2. Experimental

2.1. Materials and methods

All the chemicals were commercially obtained and used as received. The substrates for Sonogashira reactions, bases and solvents were purchased from Merck, Sigma Aldrich, LobaChemie and Rankem and 3-aminopropyltriethoxysilane (APTES) and palladium acetate were from Sigma-Aldrich. Silica gel (particle size 60–120 mesh) used for column chromatography was purchased from Rankem, India.

FT-IR spectra were recorded using KBr pellets on a Shimadzu IR Prestige-21 FT-IR spectrophotometer (400-4000 cm^{-1}). UV–vis (200–800 nm) spectra were recorded on a Jasco V-750 spectrometer in solid state. The powder XRD patterns were recorded on RikaguUltima IV diffractometer with Cu-Kα ($\lambda = 1.541$ Å) radiation. The SEM images were obtained with a JEOL, JSM IT-300 operating at an accelerating voltage of 20 kV. The EDX spectra were also recorded in the same instrument attached to the scanning electron microscope. The surface area measurement at liquid nitrogen temperature was obtained from the linear plot following Brunauer-Emmett-Teller (BET) method using Quantachrome instrument (Boynton Beach, FL 33426, USA). The X-ray photoelectron spectrum (XPS) of (Pd-imine@nanoSiO_2) was recorded on a XPS-AES Module, Model: PHI 5000 Versa Prob II. The C (1s) electron binding energy corresponding to graphitic carbon was used for calibration of the Pd (3d) core-level binding energy. Thermogravimetric analyses (TGA) were done with a Perkin Elmer STA 8000 thermal analyzer in the temperature range 35 °C-850 °C at a heating rate 20 °C min^{-1} in air. The palladium content of the catalyst was determined by Inductively Coupled Plasma Atomic Emission Spectrometric (ICP-AES) analysis with a ARCOS, Simultaneous ICP Spectrometer at SAIF, IIT Bombay. The reaction products were characterized by recording ^1H NMR spectra and comparing with authentic sample.

2.2. Synthesis of materials

Synthesis of nanosilica: From green chemistry and eco-compatibility point of view, the use of waste material is one of the major concerns in recent time. Keeping this in mind, we have used rice husk derived nanosilica [17] for immobilization of the Pd (II) complex. This process mainly involves the following steps and can be schematically represented as shown in Scheme 1. [25].

2.3. Synthesis of Pd-imine@nanoSiO_2 catalyst

Step I: Immobilization of APTES onto nanosilica (APTES@-nanoSiO_2): 4 g of nanosilica (dried at 250 °C for 20 h) was added to 100 mL of dry toluene followed by addition of APTES (0.04 g, 2.0 mmol). The resulting mixture was refluxed under N_2 for 6 h, followed by cooling, whereupon a solid product was formed. It was separated by filtration, washed repeatedly through Soxhlet extraction with toluene and finally dried at 120 °C for 24 h to obtain APTES immobilized nanosilica.

Step II: Synthesis of imine funtionalized nanosilica [imine@nanoSiO_2]: In a suspension of 2.3 g of APTES@nanoSiO_2 in 60 mL ethanol, 0.033 g (0.21 mmol) of quinoline-2-carboxyaldehyde was added and was refluxed for 6 h. A solid precipitate was formed, which was filtered off, and washed several times through Soxhlet extraction with ethanol and acetone. The resulting compound was dried at 120 °C for 24 h and designated as imine@nanoSiO_2. The amount of the imine ligand attached to the imine@nanoSiO_2 was measured from the TGA analysis and was found to be 2.14 mmol/g.

Step III: Immobilization of Pd metal onto imine funtionalized nanosilica [Pd-imine@nanoSiO_2]: 0.2 g of imine@nano-SiO_2 and 0.060 g (0.026 mmol) of $Pd(OAc)_2$ were added in 40 mL acetone and stirred at room temperature for 24 h. The product was filtered off and washed through Soxhlet extraction with acetone. The product was dried in an oven at 70 °C for 24 h, whereupon a light brown color material was obtained and was designated as Pd-imine@nanoSiO_2. The palladium content of Pd-imine@nanoSiO_2 based on ICP analysis was estimated to be 0.9 mol % per 10 mg.

2.4. Procedure for Sonogashira cross-coupling reaction

In a typical reaction, a mixture of alkyne (1.1 mmol), aryl

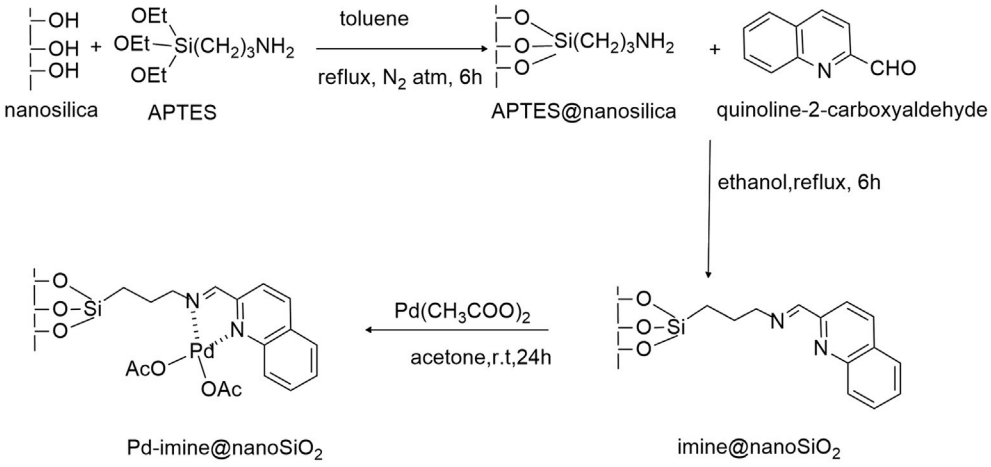

Scheme 1. Synthesis of Pd-imine@nanoSiO_2

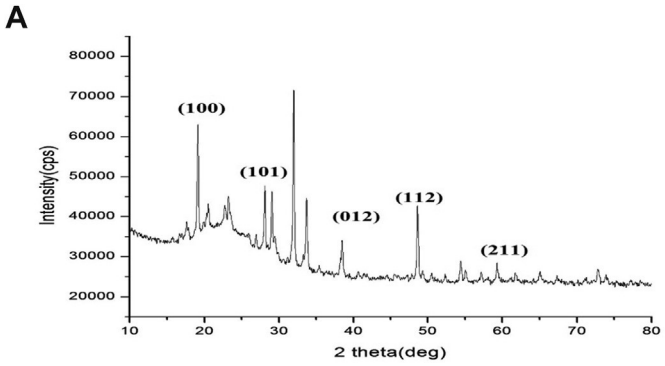

Fig. 1a. XRD pattern of silica.

halide(1.3 mmol), amine (2 mmol), catalyst (10 mg, 0.9 mol% of Pd) were added in water (4 mL) and stirred at 70 °C for required time. After completion of the reaction (monitored by GC-MS at different time intervals) it was cooled to room temperature and the catalyst was separated by simple centrifugal precipitation. The filtrated was diluted with water and extracted with 15 mL acetic acid. To obtain the desired product the organic phase was washed with brine(2×10 mL) and dried over anhydrous Na_2SO_4, then filtered and evaporated under reduced pressure. The products were isolated by silica gel column chromatography using hexane as eluent. The FT-IR and ^{1}H NMR data of isolated products were compared with previously reported literature [26,27]. To check the reusability of the catalyst, the recovered catalyst was dried overnight at 100 °C and reused in a new coupling reaction under identical conditions.

3. Results and discussion

The X-ray diffraction pattern of the complex (Fig. 1) is in good agreement with the reported literature [28–30]. The PXRD of silica exhibits peaks at 2θ value of 19.26°, 29.82°, 39.62°, 49.04° and 60.68° corresponds to (100), (101), (012), (112) and (211) planes of hexagonal unit cell [29,31]. The XRD patterns of the silica, nanosilica and the Pd-imine@nanoSiO$_2$ revealed that crystalline nature of silica changes to amorphous in both nanosilica and the complex. A broad peak corresponding to the silica phase was observed at 22° for both the materials, nanosilica and complex [25]. The XRD patterns of nanosilica and the complex are similar, however a prominent decrease in peak intensity for the complex is consistent with the immobilization of Pd and ligand onto the nanosilica as reported by Komura *et al.* [29].

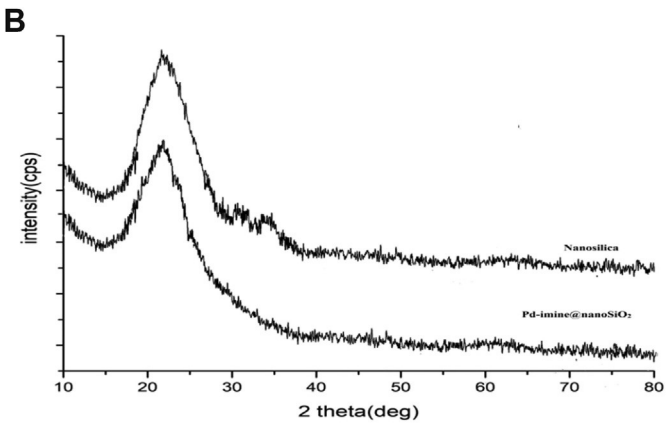

Fig. 1b. XRD patterns of nanosilica and Pd-imine@nanoSiO$_2$

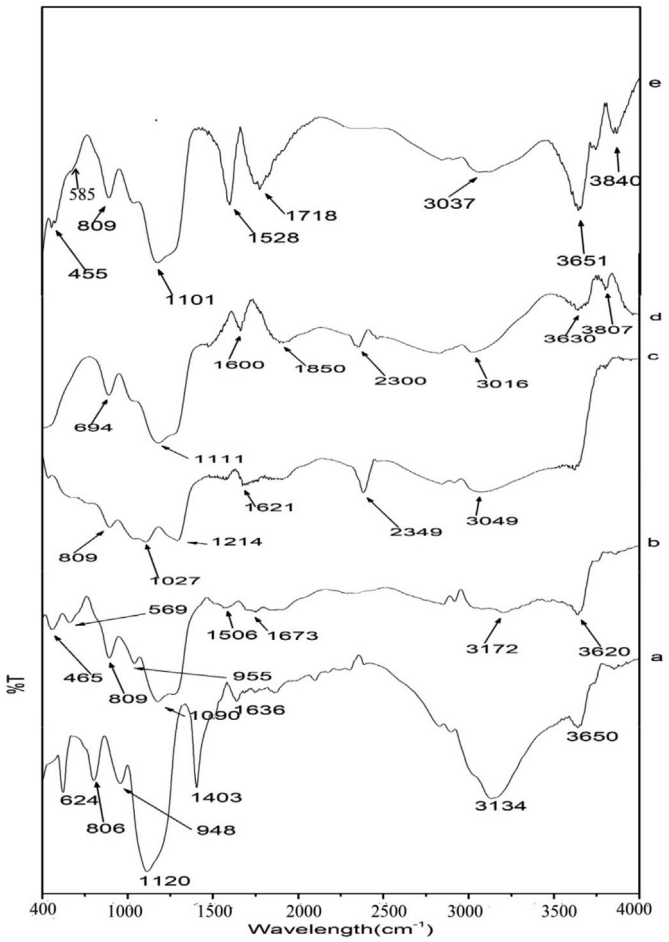

Fig. 2. FT-IR spectra of (a) silica, (b) nanosilica, (c) APTES@nanoSiO$_2$, (d) imine@nanoSiO$_2$, (e) Pd-imine@nanoSiO$_2$

FT-IR study: The FTIR spectra of nanosilica and silica are almost similar, however the bands for $\upsilon_{Si\text{-}O\text{-}Si}$, $\gamma_{Si\text{-}O\text{-}Si}$, υ_{OH} and γ_{OH} are shifted slightly either higher or lower frequency compared to that of silica(Fig. 2a and b) [23,24]. The spectrum of APTES@nanoSiO$_2$ demonstrated a peak at 1621 cm^{-1} due to γ_{NH2} indicating immobilization of APTES on nanosilica(Fig. 2c). The FTIR spectrum of imine@nanoSiO$_2$ showed a new band at 1600 cm^{-1} which could be assigned to $\nu_{C=N}$, suggesting the formation of Schiff base anchored nanosilica (Fig. 2d). Interestingly, it was observed that this band was shifted from 1600 cm^{-1} to 1528 cm^{-1}on complexation with Pd(II)(Fig. 2e). In the far-IR region a band at 455 cm^{-1}($\nu_{Pd\text{-}O}$) and 585 cm^{-1} ($\nu_{Pd\text{-}N}$) clearly suggest that Pd is coordinated through N- and O-atom [23,24].

BET analysis: With the exception of nanosilica, the surface area of silica, APTES@nanoSiO$_2$and Pd-imine@nanoSiO$_2$ decreases successively, indicating successful immobilization of APTES, imine and Pd onto the silica (Table 1). As compared to the catalysts reported by Nikoorazm et al. and Komura et al., we have observed higher

Table 1
BET surface area measurements of the silica based materials.

Entry	Materials	Surface Area(m^2/g)
1	Silica	186
2	Nanosilica	280
3	APTES@nanoSiO$_2$	135
4	Pd-imine@nanoSiO$_2$	111

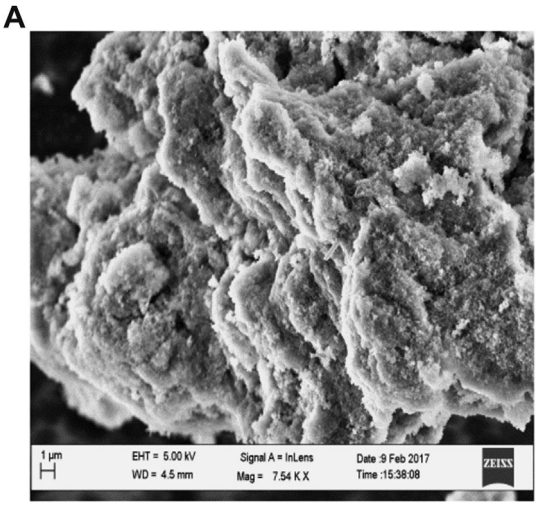

Fig. 3a. SEM image of nanosilica.

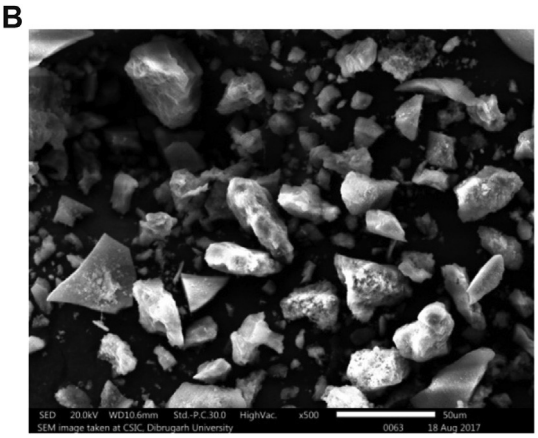

Fig. 3b. SEM image of Pd-imine@nanoSiO$_2$

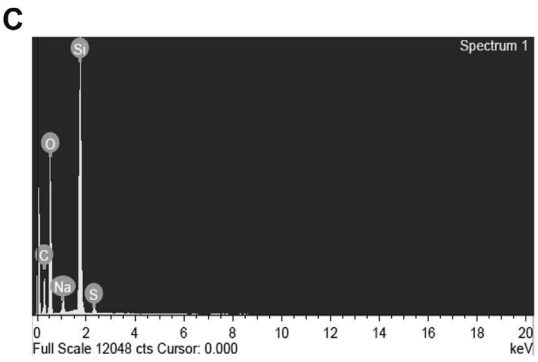

Fig. 3c. EDX of nanosilica.

decrease of surface area of nanosilica with the successive immobilization of the ligand and Pd metal [28,29].

SEM-EDX and ICP analysis: Surface morphology of nanosilica was changed after immobilization of APTES, imine and Pd onto nanosilica (Fig. 3a **&** Fig. 3b). EDX patterns of nanosilica and Pd-imine@nanoSiO$_2$(Fig. 3c **&** Fig. 3d) invariably showed the presence of Pd, N elements and suggested the successful grafting of Pd

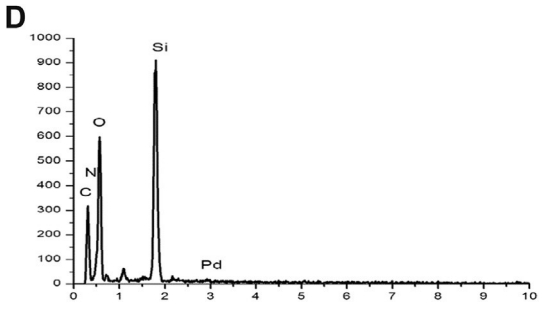

Fig. 3d. EDX of Pd-imine@nanoSiO$_2$

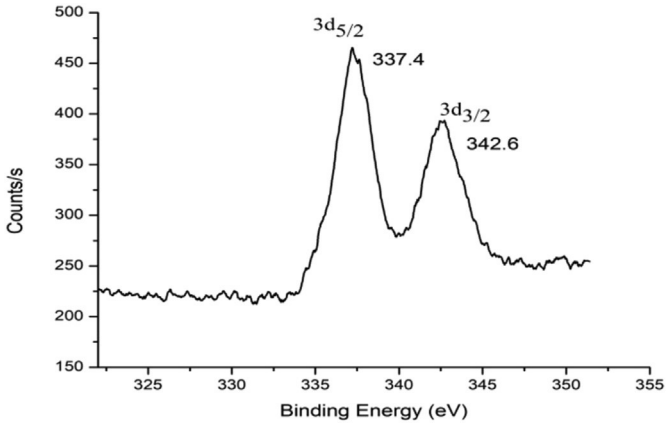

Fig. 4. Pd 3d core level XPS spectrum Pd-imine@nanoSiO$_2$

complex with the anchored ligand. ICP-AES analysis revealed 0.9 mol% of Pd content per 10 mg of Pd-imine@nanoSiO$_2$.

3.1. X-ray photoelectron spectroscopy study

The XPS study for Pd 3d core of Pd-imine@nanoSiO$_2$ is demonstrated in Fig. 4**.** The catalyst exhibited two peaks at binding energy 337.4 eV and 342.6 eV, could be assigned to the Pd^{2+} 3d core-level peaks corresponding to the palladium 5/2 and 3/2 spin-orbit components, respectively. This enumerates the presence of Pd(II)in the complex [11,28,29,32].

TGA: The TGA analysis of nanosilica, APTES@nanoSiO$_2$ and imine@nanoSiO$_2$ revealed an initial weight loss of approximately 4.5, 5.3 and 4.6%, respectively in the temperature range 100–250 °C, could be attributed to adsorbed water(Figs. S1–S3) [28,33]. With further increase in temperature the APTES@nanoSiO$_2$ and imine@nanoSiO$_2$ showed 3.80 and 5.94% wt loss corresponding to the decomposition of APTES and APTES- imine, respectively. The quantity of imine ligand attached to the Pd was measured from the TGA analysis and was found to be 2.14 wt% or 0.013 mmol in the catalyst (ESI).

UV–vis spectra: The electronic spectrum of the complex was recorded in the range 200–800 nm in solid state. The bands observed in the region 220–250 nm and 355 nm could be assigned to the intraligand transitions (Fig. 5).

3.2. Pd-imine@nanoSiO$_2$ catalyzed Sonogashira cross-coupling reaction

After characterization of the complex extensively we want to check the potentiality of the complex as a catalyst for Sonogashira

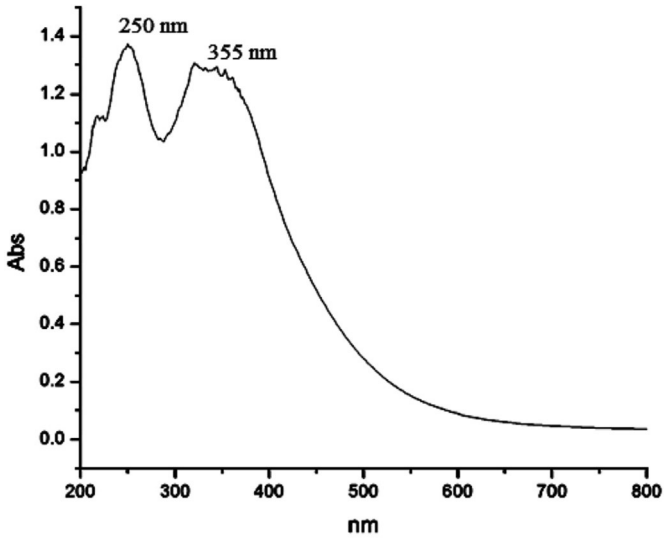

Fig. 5. Solid UV–vis spectrum for Pd-imine@nanoSiO$_2$

cross-coupling reaction with various alkynes and aryl halides. For this purpose a model reaction was carried out between phenylacetylene and iodobenzene at different temperatures using triethylamine as an additive in copper free condition (see Table 2). As we know solvent plays an important role in product formation we have screened various solvents for the reaction. From the table it is clear that water is the most suitable solvent for the reaction as other solvents gave comparatively low percentage yield (Table 2, entry1). Water may readily solvate other substrates present in the reaction medium due to high polarity index. We have also performed the reaction at different temperatures, *viz.* room temperature (25 °C), 50 °C, 70 °C, 80 °C, 100 °C and observed that 80 °C was the optimum temperature for better product yield (Table 2, entry1). Likewise, a number of runs were performed with a various amounts of Pd loadings such as 0.45, 0.9, 1.08, 1.35, 1.8 and 2.25 mol% and found that 0.9 mol% of Pd was the sufficient amount to produce the highest yield in water (Table 2, entry1). It was clear that increase of Pd loading did not improve the product yield, while decrease of Pd loading to 0.45 mol% led to decrease the yield significantly (Table 2, entries 13–17). In the absence of catalyst and solvent only trace amount of product was formed (Table 2, entries 9, 10 & 11).

Table 3
Optimization of bases for the Sonogashira cross-coupling reaction.[a].

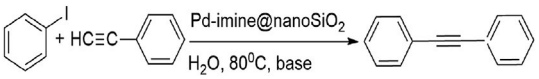

Entry	Base	Isolated yield(%)
1	K_2CO_3	60
2	$NaHCO_3$	55
3	NaOH	50
4	Et_3N	95
5	–	–
6	WEB[b]	30

[a] Reaction conditions: iodobenzene(1.0 mmol), phenyl acetylene(1.1 mmol)], H_2O(2 ml), Pd-imine@nanoSiO$_2$ (10 mg; 0.9 mol% of Pd) at 80 °C for 2 h.
[b] Water extract of banana (WEB).

Previous studies suggested that bases play a significant role in absorption of hydrogen halide in this reaction as well as inhibits the formation of homo-coupling product [34]. The reaction did not occur in absence of any base (Table 3, entry 5). We have examined both organic and inorganic bases like K_2CO_3, $NaHCO_3$, NaOH, Et_3N and water extract of banana (WEB) to find out the most efficient base for the reaction and found Et_3N as the most efficient base for the reaction (Table 3, entry 4). This might be due to the fact that amines trap hydrogen halide readily compared to inorganic bases [35,36]. The results are summarized in the Table-3.

To widen the scope of the reaction we have carried out Sonogashira cross-coupling reaction between a wide range of

Table 2
Optimization of the reaction conditions for the Sonogashira reaction of phenyl acetylene and iodobenzene using Pd-imine@nanoSiO$_2$ as a catalyst [a]

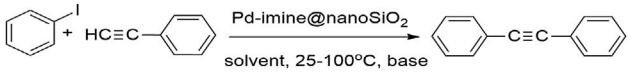

Entry	Solvent	Catalyst (mg; Pd loading)	Temperature(°C)	Time (h)[b]	Isolated yield(%)
1	H_2O	10 (0.9 mol% Pd)	80	2	95
2	Isopropanol	10 (″)	80	2	65
3	DMF	10(″)	80	2	55
4	EtOH	10(″)	80	4	50
5	CH_3CN	10(″)	80	2	70
6	EtOH/H_2O	10(″)	100	3	85
7	H_2O	10(″)	25 (r.t.)	24	trace
8	H_2O	10(″)	50	4	60
9	H_2O	–	100	2	trace
10	H_2O	–	100	4	trace
11	–	10(″)	100	24	trace
12	H_2O	10(″)	70	4	80
13	H_2O	5(0.45 mol% Pd)	80	5	65
14	H_2O	12(1.08 mol% Pd)	80	2	95
15	H_2O	15(1.35 mol% Pd)	80	2	95
16	H_2O	20(1.80 mol% Pd)	80	2	95
17	H_2O	25(2.25 mol% Pd)	80	2	95

[a] Reaction conditions: Aryl halide (1.3 mmol), phenyl acetylene (1.0 mmol), triethylamine (2.0 mmol), catalyst (Pd-imine@nanoSiO$_2$) and solvent (3 ml).
[b] All reactions were carried out for 24 h however, the time required to get maximum conversion is reported here.

Table 4
Sonogashira cross-coupling reactions of different aryl halides and alkynes in water.[a].

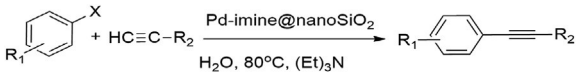

Entry	Aryl halide	Alkyne	Product	Isolated yield (%)
1		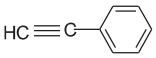		85
2	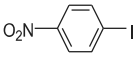	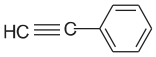	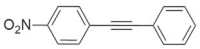	80
3	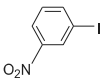	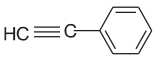	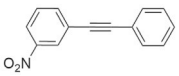	75
4		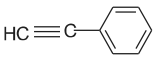	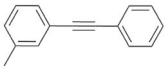	92
5		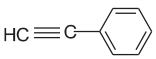	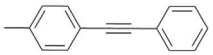	96
6		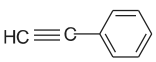	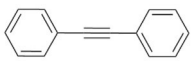	85
7		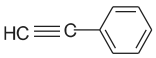	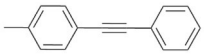	87
8		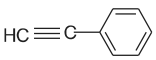	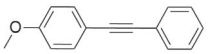	85
9	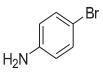	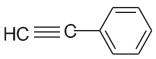	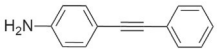	88
10		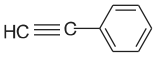	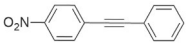	77
11		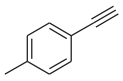	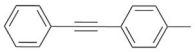	90
12	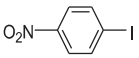	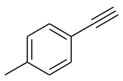	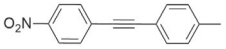	85
13	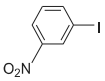	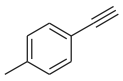	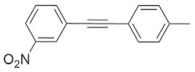	87
14		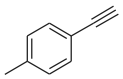	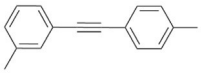	85
15		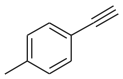	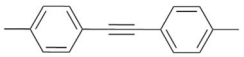	90
16		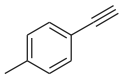	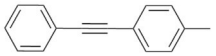	80
17		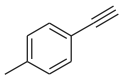		82
18		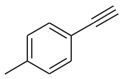	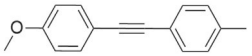	77
19	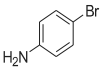	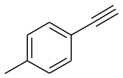	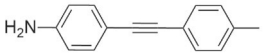	81

(*continued on next page*)

Table 4 (*continued*)

Entry	Aryl halide	Alkyne	Product	Isolated yield (%)
20		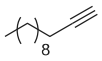	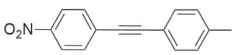	81
21		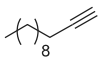	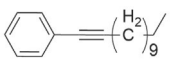	78
22	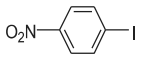	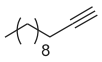	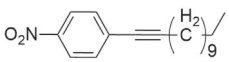	80
23	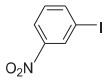	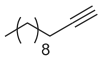	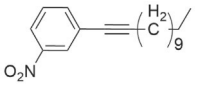	78
24		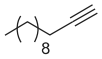	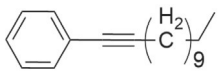	73
25		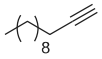	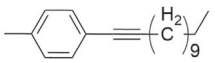	75

[a] Reaction conditions: aryl halide(1.0 mmol), alkyne(1.1 mmol), Pd-imine@nanoSiO$_2$(10 mg; 0.9 mol% of Pd),Et$_3$N(2.0 mmol), H$_2$O (2 ml).

substrates with Pd-imine@nanoSiO$_2$ as the catalyst. Water as a solvent tolerates very hardly both aryl iodides and aryl bromides as substrate to give good yield, however our catalytic system showed high tolerance for both aryl iodides and aryl bromides. Aryl bromides gave comparatively lower isolated yield than the aryl iodides (Table 4, entries 6–10 & 16–20) and aryl iodides with electron donating groups gave higher yield compared to electron withdrawing groups (Table 4, entries 4,5&15). Aliphatic alkynes coupled less effectively with aryl halides and afforded low yields, might be attributed to the presence of less acidic terminal hydrogen which results slow coordination of alkyne to aryl palladium intermediate to form aryl alkynyl palladium species (Table 4, entries 20–25).

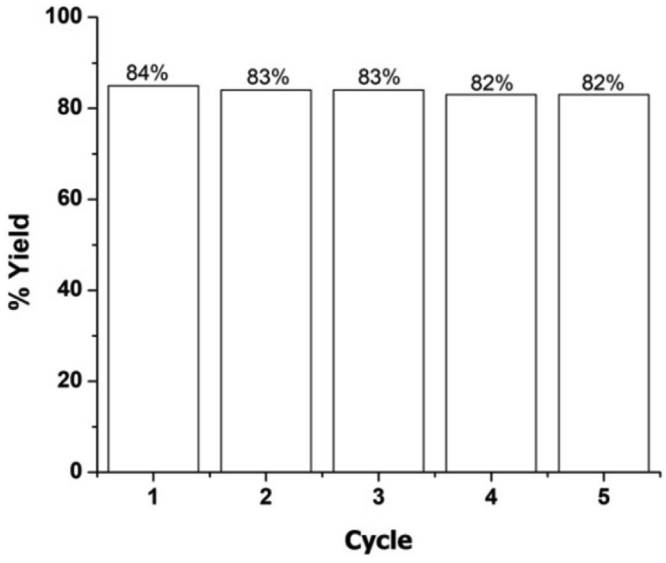

Fig. 6. Reusability of Pd-imine@nanoSiO$_2$ in the Sonogashira cross-coupling reaction. Reaction conditions: Catalyst (10 mg; 0.9 mol %); iodobenzene (6.3 mmol); phenyl acetylene (6.0 mmol); (Et)$_3$N (12 mmol); H$_2$O (9 ml); temperature: 80 °C.

3.3. Catalyst leaching and reusability of the catalyst

3.3.1. Hot filtration test

We have carried out a hot filtration test to know whether these catalytic reactions are truly heterogeneous or not by using phenyl acetylene and iodobenzene in the presence of Pd-imine@nanoSiO$_2$ catalyst (10 mg; 0.9 mol% of Pd) and stirred at 80 °C. After 30 min the reaction was stopped and the catalyst was filtered off (55% yield found from GC-MS). The reaction was allowed to progress without the catalyst for another 1 and 1/2 h, which eventually showed no increase in product yield. This clearly suggested non-leaching of Pd during reaction which was further confirmed by ICP-AES analysis with the filtrate.

3.3.2. Reusability test

Retrievability of a catalyst is of utmost concern to evaluate

Fig. 7a. SEM of catalyst after 5th cycle.

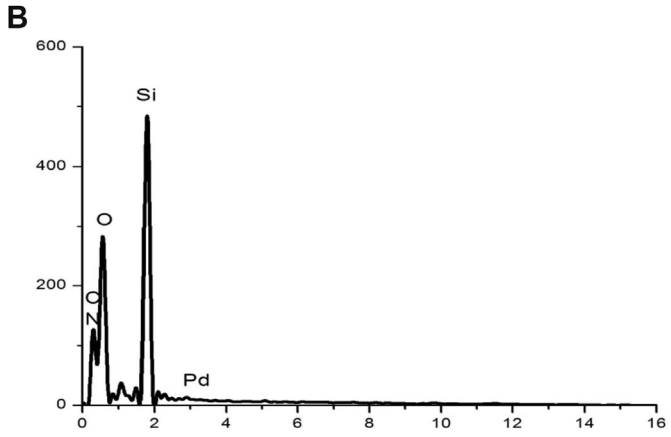

Fig. 7b. EDX spectrum of the catalyst.

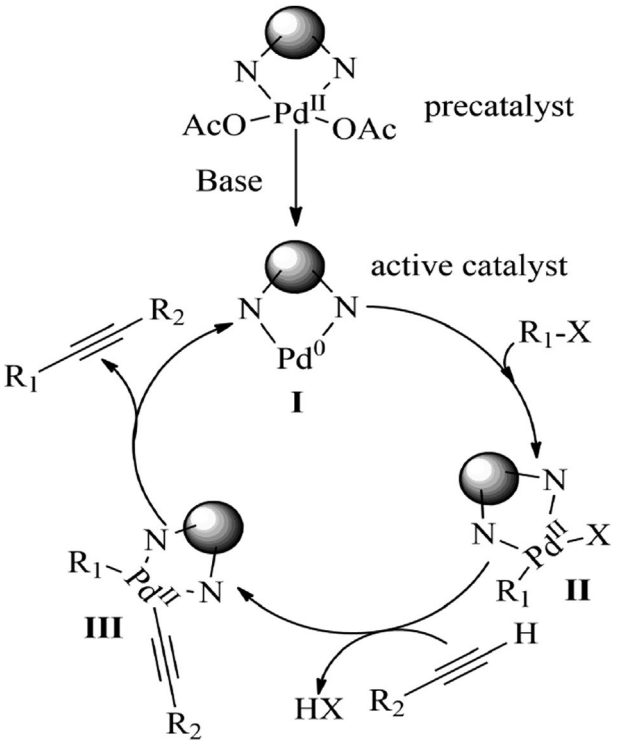

Scheme 2. The probable mechanism of copper free Sonogashira reaction.

the efficiency of the catalyst as well as from the economic point of view. We therefore conducted the recyclability experiment by taking iodobenzene and phenyl acetylene as coupling partners with 10 mg (0.9 mol% of Pd) of the catalyst. After completion of the reaction (monitored by GC-MS) the catalyst was separated with centrifugal precipitation and dried at temperature 120 °C in an oven for 24 h. Then the catalyst was reused in a new coupling reaction. To our delight the catalyst showed good recyclability for five consecutive runs without significant loss in activity (Fig. 6).

To check the chemical change of the catalyst during subsequent runs we have performed a SEM-EDX analysis of the catalyst recovered after the fifth catalytic cycle (Fig. 7a & b). It revealed that the catalyst retains its initial chemical composition even after 5th catalytic cycle.

A plausible mechanism for the catalytic performance of Pd-imine@nanoSiO_2 in copper free condition for Sonogashira reaction is demonstrated in Scheme 2. In analogy with the earlier reports, the mechanism initially may be started with the activation of Pd-imine@nanoSiO_2 and generating acetate free Pd(0) real catalytic species **I** in basic medium [4]. This was followed by the oxidative addition of aryl halide to the species **I** through the oxidation of Pd(0) to Pd(II). The coordination of terminal alkyne to intermediate **II** producing palladium acetylide complex **III** . At the final step Sonogashira reaction product was released through the reductive elimination of complex **III** with the simultaneous release of the active catalyst for the next catalytic cycle. To confirm the nature of the real catalytic species we have recorded TEM image of the catalyst after completion of the reaction, which clearly showed the formation of Pd(0) nanoparticles (Fig. S4).

To know the actual catalytic performance of our catalyst with respect to the reported ones we have performed a literature survey (Table 5) and our catalyst was found to be effective with wide substrate scope at mild reaction conditions.

4. Conclusion

We have developed an eco-friendly, novel protocol for Sonogashira cross-coupling reaction using Pd-imine@nanoSiO_2. The catalyst exhibited excellent catalytic efficiency for carbon-carbon triple bond activation reactions between arylhalides(both iodides and aryl bromides) and terminal alkynes in water. Our catalyst could be easily recovered from the reaction mixture by simple centrifugal precipitation and reused for five consecutive catalytic cycles without profound loss in activity. This protocol is also moderately suitable for aliphatic alkynes.

Table 5
Comparative study on Sonogashira cross-coupling reactions with different catalytic systems.

Catalyst	Reaction Conditions	Yield/Conversion (%)	Literature reference
Pd(II)Cl_2-BTP@TMSP-nSiO_2	DIPEA, DMF/H_2O,RT, 2–3 h,0.15 mol%	80–95	[4]
Nano-Pd(0)/SDPP	K_2CO_3, PEG 200, 100 °C, 1.5–4 h,0.5 mol%	50–91	[3]
Pd-LHMS-3	Hexamine, H_2O, reflux, 10–15 h,0.52 mol%	70–90	[2]
nSiO_2-Dendrimer-Pd(0)0	$(Et)_3N$,H_2O,reflux,4–12 h, 0.085 mol%	82–96	[5]
Pd-2QC-MCM	Piperidinen,NMP,80 °C, 3 h,1.8 mol%	49–100	[29]
Pd-ABA-MCM-41	K_2CO_3, PEG 200, 60 °C,1–7 h,1.6 mol%	92–97	[28]
CuNPs@MP-3	Et_3N, H_2O, 40 °C, 8 h,1 mol%	70–96	[35]
Co-MS@MNPs/CS	KOH,DMSO,140 °C,10–12 h, 1.1 mol %	45–80	[37]
Pd/ICCP	K_2CO_3,EtOH,100 °C,4 h, 1 mol %	64–92	[38]
Pd-BIP-γ-Fe_2O_3@SiO_2	Et_3N,DMF,100 °C,1.5–6 h,0.5 mol %	71–96	[39]
Pd(II)-PMO-SBA-16	DBU,CuI,H_2O,90 °C,4–10 h, 0.9 mol %	85–93	[40]
Pd-imine@nanoSiO_2	$(Et)_3N$, H_2O, 80 °C,2 h, 0.9 mol%	50–97	Our work

Acknowledgments

The authors thank SAIF, STIC, Kochi University, Kochi for ICP-AES analysis, SAIF, NEHU, Shillong for ^{1}H NMR facilities and ACMS, IIT Kanpur for X-ray photoelectron spectroscopic analytical facilities. The authors express their gratitude to UGC, New Delhi for the SAP-DRS-I grant (2016–2021) awarded to the department of Chemistry, Dibrugarh University.

Appendix A. Supplementary data

Supplementary data to this article can be found online at https://doi.org/10.1016/j.jorganchem.2019.06.015.

References

[1] A. Gogoi, A. Dewan, G. Borah, U. Bora, New J. Chem. 39 (2015) 3341.
[2] A. Modak, J. Mondal, A. Bhaumik, Green Chem. 14 (2012) 2840.
[3] N. Iranpoor, B.H. Firouzabadi, B.S. Motevalli, Aust. J. Chem. 68 (2015) 926.
[4] Z. Dehbanipour, M. Moghadam, S. Tangestaninejad, V. Mirkhani, I. Mohammadpoor-Baltork, J. Organomet. Chem. 853 (2017) 5.
[5] M. Esmaeilpour, A. Sardarian, J. Javidi, Catal. Sci. Technol. 6 (2016) 4005.
[6] M. Lamblin, L. Nassar-Hardy, J.C. Hierso, E. Fouquet, F.X. Felpin, Adv. Synth. Catal. 352 (2010) 33.
[7] Z. Mandegani, M. Asadi, Z. Asadi, Appl. Organomet. Chem. 30 (2016) 657.
[8] W. He, F. Zhang, H. Li, Chem. Sci. 2 (2011) 961.
[9] S.N. Jadhav, A.S. Kumbhar, S.S. Mali, C.K. Hong, R.S. Salunkhe, New J. Chem. 39 (2015) 2333.
[10] P. Veerakumar, P. Thanasekaran, K.L. Lu, S. Bin Liu, S. Rajagopal, ACS Sustain. Chem. Eng. 5 (2017) 6357.
[11] J. Baruah, R. Gogoi, N. Gogoi, G. Borah, Transit. Met. Chem. 42 (2017).
[12] J.H. Kim, J.W. Kim, M. Shokouhimehr, Y.S. Lee, J. Org. Chem. 70 (2005) 6714.
[13] M. Bakherad, A. Keivanloo, S. Samangooei, Chin. J. Catal. 35 (2014) 324.
[14] M. Navidi, N. Rezaei, B. Movassagh, J. Organomet. Chem. 743 (2013) 63.
[15] S.M. Sarkar, M.M. Yusoff, M.L. Rahman, J. Chin. Chem. Soc. 62 (2015) 33.
[16] S. Diyarbak, H. Can, O. Metin, Appl. Mater. Interfaces 7 (2015) 3199.
[17] A. Khalafi-Nezhad, F. Panahi, Green Chem. 13 (2011) 2408.
[18] D.A. Kotadia, U.H. Patel, S. Gandhi, S.S. Soni, RSC Adv. 4 (2014) 32826.
[19] M. Opanasenko, P. Stepnicka, J. Cejka, RSC Adv. 4 (2014) 65137.
[20] M. Pagliaro, V. Pandarus, F. Béland, R. Ciriminna, G. Palmisano, P.D. Carà, Catal. Sci. Technol. 1 (2011) 736.
[21] N. Pal, A. Bhaumik, RSC Adv. 5 (2015) 24363.
[22] S. Cui, S. Yu, B. Lin, X. Shen, X. Zhang, D. Gu, J. Porous Mater. 24 (2017) 455.
[23] N. Gogoi, U. Bora, G. Borah, P.K. Gogoi, Appl. Organomet. Chem. 31 (2017) 1.
[24] S. Sultana, G. Borah, P.K. Gogoi, Appl. Organomet. Chem. 33 (2018), https://doi.org/10.1002/aoc.4595.
[25] N. Gogoi, T. Begum, S. Dutta, U. Bora, P.K. Gogoi, RSC Adv. 5 (2015) 95344.
[26] Q. Zhu, L. Liao, G. Cheng, W. Yang, Y. Deng, D. Yang, Mod. Res. Catal. 06 (2017) 121.
[27] B.N. Lin, S.H. Huang, W.Y. Wu, C.Y. Mou, F.Y. Tsai, Molecules 15 (2010) 9157.
[28] M. Nikoorazm, N. Noori, B. Tahmasbi, S. Faryadi, Transit. Met. Chem. 42 (2017) 469.
[29] K. Komura, H. Nakamura, Y. Sugi, J. Mol. Catal. A Chem. 293 (2008) 72.
[30] P. Wang, G.Y. Wang, W.L. Qiao, Y.S. Feng, Catal. Lett. 146 (2016) 1792.
[31] M. Mishra, A.P. Singh, P. Sambyal, S.K. Dhawan, Indian J. Pure Appl. Phys. 52 (2015) 478.
[32] Y.H. Ng, M. Wang, H. Han, C.L.L. Chai, Chem. Commun. 0 (2009) 5530.
[33] R. Kotcherlakota, A.K. Barui, S. Prashar, M. Fajardo, D. Briones, A. Rodríguez-Diéguez, C.R. Patra, S. Gómez-Ruiz, Biomater. Sci. 4 (2016) 448.
[34] T. Ljungdahl, T. Bennur, A. Dallas, H. Emtenäs, J. Mårtensson, Organometallics 27 (2008) 2490.
[35] K. Wang, L. Yang, W. Zhao, L. Cao, Z. Sun, F. Zhang, Green Chem. 19 (2017) 1949.
[36] M. Bakherad, Appl. Organomet. Chem. 27 (2013) 125.
[37] A.R. Hajipour, F. Rezaei, Z. Khorsandi, Green Chem. 19 (2017) 1353.
[38] T. Saetan, C. Lertvachirapaiboon, S. Ekgasit, M. Sukwattanasinitt, S. Wacharasindhu, Chem. Asian J. 12 (2017) 2221.
[39] S. Sobhani, Z. Zeraatkar, F. Zarifi, New J. Chem. 39 (2015) 7076.
[40] F. Zhu, L. Zhu, X. Sun, L. An, P. Zhao, H. Li, New J. Chem. 38 (2014) 4594.